

## Lens mount for cryogenic refractive optics cooled by mechanical cryocooler

Wang Zhaoli<sup>1,2</sup>, Liang Jingtao<sup>1</sup>, Zhao Miguang<sup>1</sup>, Chen Houlei<sup>1</sup>, Wang Juan<sup>1</sup>, Wei Lingjiao<sup>1</sup>

(1. Key Laboratory of Space Energy Conversion Technology, Technical Institute of Physics and Chemistry, Chinese Academy of Sciences, Beijing 100190, China; 2. University of Chinese Academy of Sciences, Beijing 100049, China)

**Abstract:** In practical application, cryogenic optics can effectively improve the detection sensitivity by reducing the thermal noise of the infrared optical system. The lens mount is a key component to ensure the normal performance of the cryogenic optical system at cryogenic temperature. A transmission optical system was designed to work at the operation temperature of 150 K where the pulse tube cryocooler was used as a novel mechanical cryocooler to cool the optics. However, due to the small diameter of the pulse tube cryocooler's cold finger, the temperature difference within the lens was large when it was connected directly with the cold finger. So the lens needs to be cooled via a properly designed mount. Specialized axial support and radial support were designed to prevent from making damages and large distortion of the lens at cryogenic temperature. The heat transfer model between the lens and the pulse tube cryocooler was established to guide the lens mount thermal design. Finally, the cryogenic performance of the lens mount was tested. The experimental results showed that in about three hours, the optical components survived the cool-down process from the initial temperature of 300 K to the operation temperature of 150 K, and the maximum temperature difference within the lens was less than 1 K. The distortion test showed the maximum deformation of the optical surface was less than  $1 \lambda$  ( $1 \lambda=632.8 \text{ nm}$ ) when the temperature decreased from 300 K to 150 K. The designed lens mount successfully satisfies the requirements of this cryogenic optical system which provides a new choice for the cryogenic optics cooled by mechanical cryocooler.

**Key words:** cryogenic optics; lens mount; temperature difference; pulse tube cryocooler; IR imaging

**CLC number:** TN216 **Document code:** A **DOI:** 10.3788/IRLA201948.0218006

## 机械制冷机冷却的透射式光学系统支撑结构

王兆利<sup>1,2</sup>, 梁惊涛<sup>1</sup>, 赵密广<sup>1</sup>, 陈厚磊<sup>1</sup>, 王娟<sup>1</sup>, 卫铃佼<sup>1</sup>

(1. 中国科学院理化技术研究所 空间功热转换技术重点实验室, 北京 100190;  
2. 中国科学院大学, 北京 100049)

收稿日期: 2018-09-07; 修订日期: 2018-10-12

基金项目: 中国科学院国防创新基金(CXJJ-17-M133); 科技部重点研发计划(2016YFB05500501)

作者简介: 王兆利(1988-), 男, 博士生, 主要从事空间制冷及低温光学方面的研究。Email: wangzhaoli@mail.ipc.ac.cn

导师简介: 梁惊涛(1965-), 男, 研究员, 博士生导师, 博士, 主要从事脉冲管制冷机方面的研究工作。Email: jtliang@mail.ipc.ac.cn

**摘要:** 低温光学能够降低红外光学系统自身热噪声,有效提高探测灵敏度。支撑结构是实现光学系统在低温下正常工作的关键部件。设计的透射式低温光学系统工作温度为 150 K,采用脉冲管制冷机这种新型机械式低温制冷机做冷源。因制冷机冷指直径较小,直接冷却光学透镜会在透镜内部产生较大温差,影响成像质量,为此设计了一种新型支撑结构,一方面设计了新型的轴向支撑和径向支撑用来减少透镜在低温下的形变,另一方面建立了透镜与脉冲管制冷机之间的传热模型,来指导支撑结构热设计,减小透镜内部温差。最后,对透镜支撑的低温性能进行了测试,实验结果表明,经过 3 h,透镜温度由 300 K 降至 150 K,支撑结构很好地保护了透镜并且在降温过程中透镜内部温差小于 1 K。当温度从 300 K 降低到 150 K 时,光学表面的最大变形小于  $1 \lambda$  ( $1 \lambda = 632.8 \text{ nm}$ )。支撑结构从机械和热学性能上满足了低温光学系统的需要,为机械式制冷机冷却光学系统的光机结构设计提供了一种新选择。

**关键词:** 低温光学; 透镜支撑; 温度梯度; 脉冲管制冷机; 红外成像

## 0 Introduction

The final performance of the infrared instruments depends strongly on the minimization of the instrumental thermal background radiation. In order to keep this internal thermal background radiation as low as possible, IR instruments are usually cooled to cryogenic temperatures which is at or below liquid nitrogen temperature (77 K)<sup>[1-5]</sup>. Cryogenic optics has played an important role in infrared applications especially in the ground or space based telescope and interferometer. For ground based application, lenses of Omega2000 were cooled to a temperature of about 77 K by liquid nitrogen<sup>[6]</sup>. Integral field spectrograph (IFS) optics in the Gemini Planet Imager (GPI) was composed of 8 lenses. All lenses were equipped with a mechanical cryocooler and tested at 80 K<sup>[7]</sup>. All optics of the mid infrared instrument (MIDI) of the Very Large Telescope Interferometer (VLTI) were cooled to 40 K by a closed cycle cooler<sup>[8]</sup>. For space application, there are numbers of well-known examples of major civilian cryogenic telescopes which have been developed, launched and achieved successful performance in scientific investigations. Both the Infrared Astronomical Satellite (IRAS) and the Infrared Space Observatory (ISO) telescope were cooled to

4 K using on-board liquid helium<sup>[9]</sup>. Lenses of the Near Infrared Camera (NIRCam) in the James Webb Space Telescope (JWST) were cooled to 35 K via deep space radiators<sup>[10]</sup>. The whole telescope system of ASTRO-F was cooled down to 5.8 K with a combined use of super-fluid liquid helium and mechanical coolers<sup>[11]</sup>.

Optical systems, cryogenic cold sources, and opto-mechanical structures are the main components in these cryogenic optical systems as mentioned above. Cryogenic optics can be briefly divided into two categories: refractive and reflective optics. Refraction optical system has the characteristics of small size, large field of view and simple loading, making it possible to be used in the situations with volume and weight constraints. In this study, refractive optics was used in cryogenic optics. However, as refractive index of infrared optics materials and optical surface deformation are sensitive to the temperature variation, special attentions are needed to the temperature control of the optical system.

The methods to cool down the optics are liquid cryogenics, passive radiator and mechanical cryocooler. Compared with traditional cryogenic optics cooled by cryogenics, the optics system cooled by mechanical refrigerators can reduce the weight and size immensely. The traditional

mechanical refrigerators that can be used to cool the optical system are Stirling refrigerators and GM refrigerators. As their cold heads have moving parts, and the resulting vibrations have an effect on the optical system, limiting their application in high-sensitivity detection. With the development of the cryogenic technology, the refrigerating capacity of pulse tube cryocooler as a novel mechanical cryocooler is becoming larger and larger, due to the absence of moving parts in the cold finger of pulse tube cryocooler, it has little interference with the optical system, making it a new mechanical cryocooler to cool optical system. However, just as the other mechanical cryocoolers, the diameter of the pulse tube cryocooler's cold finger is pretty smaller than that of the lens, if the cold finger were connected directly to the large lens, it would create great temperature gradient within the lens, which could even break the lens. Therefore, in order to solve this problem, a novel structure of the lens mount is designed and analyzed in this study, which is focused on optimizing the thermal behavior of the mount to decrease temperature gradient within the lens and limiting the distortion of the lens.

### 1 Lens design

The optical system was designed as a prototype to verify the possibility of the cryogenic optics cooled by the pulse tube cryocooler. For this reason, the limitation of the detector is a major factor in the process of lens design. The detector used in this cryogenic optical system is a HgCdTe focal plane array detector with 320 pixel×256 pixel and the single pixel size is 30 μm×30 μm. The imaging spectral band of the detector is 8–12 μm and the detector Dewar *F* number is 2. According to the law of blackbody radiation, the radiation intensity is

proportional to the fourth power of the temperature. The slope of the curve of the radiation intensity with temperature becomes quite small in the lower cryogenic temperature region especially below temperature of 150 K. As the temperature further decreases, the benefit in performance by cooling optics is not obvious, but the increase of the cryocooler input power is giant. Hence, as a prototype of cryogenic optics, the operating temperature is chosen to be 150 K.

The optical system was designed to image from 8 to 12 μm by using Zemax software. The optical layout is illustrated in Fig.1. The camera consists of a three-lens triplet with a nearly 70 mm

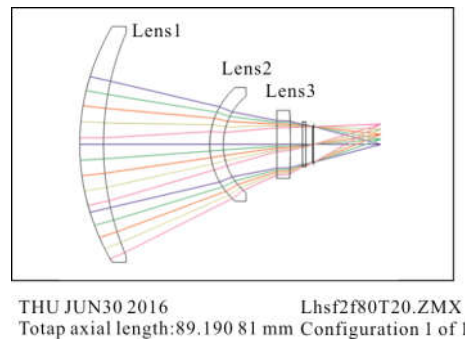


Fig.1 Layout of the optics

clear aperture while the focal length is 80 mm. The three lenses which are made of Ge, ZnS and Ge respectively can allow for large color spectrum required by the operation. All of the lenses are anti-reflection coated to improve the performance and to protect the lens substrates. All of the surfaces of the three lenses are spherical, except for one mild aspheric surface on the first Ge lens which is diamond turned to precisely match the lens specifications. The system was designed to be optimized at 10 μm with a 8.8° diagonal field of view and the average MTF value of the full field of view exceeded 0.5, which approached the diffraction limit, as shown in Fig.2.

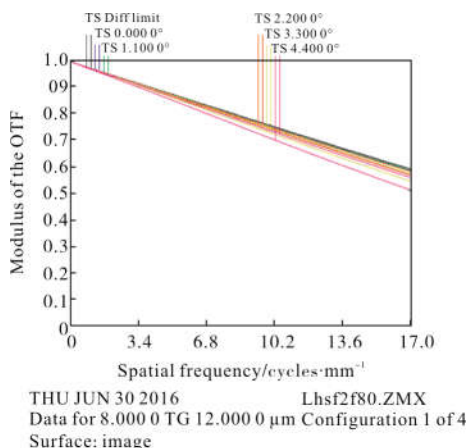
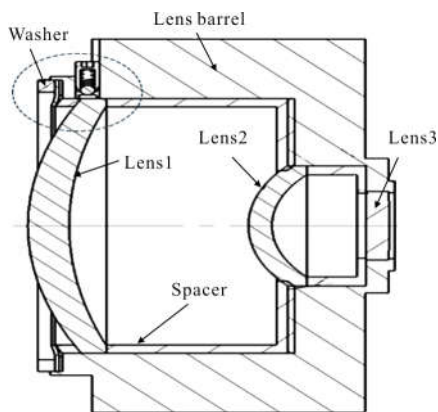


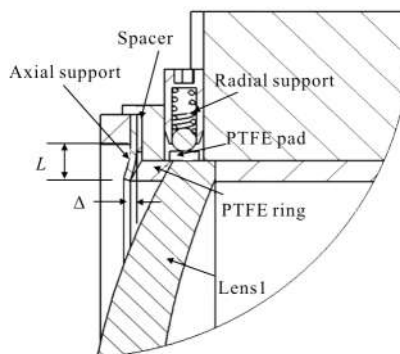
Fig.2 Results of MTF analysis

## 2 Lens mount mechanical design

Due to the different thermal contraction of the lens and the mount, mounting optics for a cryogenic optical system is a challenging undertaking. The mount should ensure the lens in stable condition and well-known position, and maintain excellent optical surface quality while going through a differential thermal contraction when the temperature drops from ambient temperature to cryogenic temperature. For the purpose of overcoming this challenge, a lens mount with novel structure is designed in this paper, as illustrated in Fig.3. The lens mount consists of lens barrel, lenses, spacers, washer, radial support, axial support, and PTFE (Poly Tetra Fluor Ethylene) ring. The spacers employ spherical surface to maximize contact area and minimize contact stress.



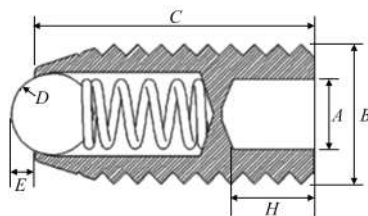
(a) Cut-away view of the design



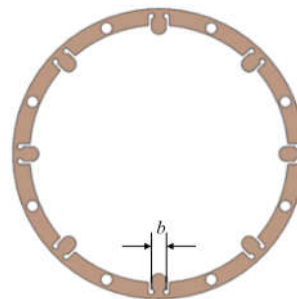
(b) Partial enlargement view of the design

Fig.3 Schematics of the lens mount

The radial aspect of the mounting consists of 3 spring screws with 120° intervals around the lens. Details of the spring assembly are shown in Fig.4(a). Compared to the traditional flexural mounts which have high fabrication cost, this mount is simpler in structure and lower in cost. Radial support stress is adjusted by springs at room temperature, which can be adjusted as needed to find the proper preload to keep the lens in the center.



(a) Radial support



(b) Axial support

Fig.4 Photograph of the support for holding the lens

In this design, the lens radial support is provided only by three spring screws, and the lens barrel should not produce stress on the optical

element during the cooling process. Hence, the radial clearance between the lens and the mount should be within reasonable limits. Taking lens1 as an example, as the material of the lens and the lens barrel is germanium and aluminum respectively, a drop in temperature will cause the mount to contract radially toward the optic's rim. Radial clearance between these components will decrease in size and, if the temperature falls far enough, the inner diameter of the mount will contact the outer diameter of the optic. Then, further temperature decrease causes radial force to be exerted upon the rim of the optic. This force compresses the optic radially and creates radial stress. If the radial clearance is too large, it is difficult to adjust the lens to the center position. Considering the manufacture and assembly conditions, the radial clearance can be set as 0.1 mm. The stress on the optical element produced by the lens barrel during the cooling can be evaluated by<sup>[12]</sup>:

$$S_R = -K_4 \cdot K_5 \cdot \Delta T \quad (1)$$

where

$$K_4 = \frac{\alpha_M - \alpha_G}{\frac{1}{E_G} + \frac{D_G}{2 \cdot E_M \cdot t_c}} \quad (2)$$

$$K_5 = 1 + \frac{2\Delta r}{D_G \cdot \Delta T (\alpha_M - \alpha_G)} \quad (3)$$

where  $D_G$  is the optic outer diameter,  $t_c$  is the mount wall thickness directly outside the rim of the optic, and  $\Delta r$  is the radial clearance.  $\alpha_G$  and  $\alpha_M$  are the CTEs of the optical materials and the mount respectively,  $E_M$  and  $E_G$  are Young's modulus for optical materials and the mount respectively.  $\Delta T$  is the temperature change. In this design, the diameter of lens1 is 70 mm which is mounted in a lens cell machined to provide 0.1 mm of radial clearance for the assembly at room temperature. The cell wall thickness is 5.5 mm.  $E_G = 10.27 \times 10^{10}$  Pa,  $\alpha_G = 5.5 \times 10^{-6}/K$ ,  $E_M = 7.05 \times 10^{10}$  Pa,  $\alpha_M = 2.313 \times 10^{-5}/K$ <sup>[13]</sup>,

$\Delta T = 150 K - 300 K = -150 K$ . According to Eq.(1), the radial compressive stress  $S_R$  developed in the lens is  $-5.28$  MPa at 150 K. This negative radial stress is resulted from the fact that the CTE difference is insufficient to cause lens rim-to-cell inner diameter contact at cryogenic temperature. Based on Eq. (3), the temperature at which no radial stress is developed can be calculated by:

$$\Delta T = \frac{2\Delta r}{D_G \cdot (\alpha_M - \alpha_G)} \quad (4)$$

In this design,  $\Delta T$  is equal to 162 K, which means no radial stress is developed at 138 K when the room temperature is 300 K.

Axial support is provided by an annular BeCu spring which is attached to the lens mount by several screws penetrating through an aluminum washer. The inner portion of the spring is slit radially to form 8 independently acting cantilevered springs, as shown in Fig.4(b). Deflections of these springs preload the lens against a shoulder of the lens barrel. The magnitude of each deflection is adjusted by machining the thickness of an aluminum ring which is located between the spring and the lens barrel. The spring thickness is 0.3 mm. The spring deflection is 1 mm. When the temperature changes, the spring deflection changes slightly so as to maintain nearly constant axial preload on the lens. The axial preload can be calculated by<sup>[12]</sup>:

$$P = \frac{\Delta \cdot E_M \cdot b \cdot t^3 \cdot N}{4 \cdot L^3 (1 - \nu_M^2)} \quad (5)$$

where  $\nu_M$  is Poisson's ratio for the clip material,  $\Delta$  is the deflection,  $L$  is the free length of the clip,  $E_M$  is Young's modulus for the material,  $b$  is the width of the clip,  $t$  is the thickness of the clip, and  $N$  is the number of clips. In this support structure,  $\Delta = 1$  mm,  $L = 5.8$  mm,  $b = 4$  mm,  $t = 0.3$  mm,  $N = 8$ ,  $E_M = 13.3 \times 10^{10}$  Pa,  $\nu_M = 0.35$ . According to Eq.(5), the axial preload  $P$  is calculated to be 167.8 N.

In this part, the effects of radial support and axial support are numerical simulated. When the temperature changes, corresponding distortion occurs on the optical surface, which can be analyzed using ANSYS. The mechanical load including radial stress and axial preload is applied to the lens. The thermal condition that the temperature decreases from room temperature 300 K to 150 K ( $\Delta T=150$  K) is loaded. According to the simulation results, the maximum distortion of the first surface of lens1 during the cooling is predicted to be  $1 \lambda$  peak-to-valley ( $1 \lambda=632.8$  nm), as shown in Fig.5. This distortion would have little influence on the image quality.

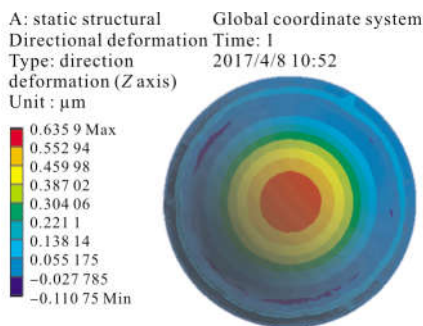
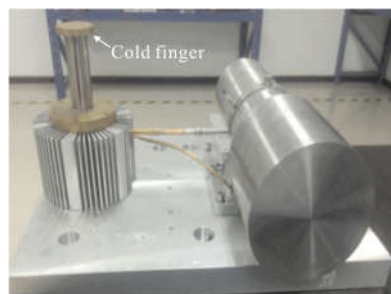


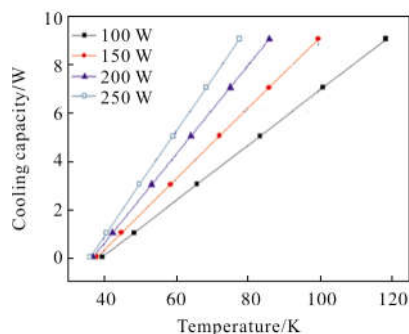
Fig.5 Surface1 distortion of lens1

### 3 Lens mount thermal design

The optics system cooled by mechanical refrigerators can reduce the weight and size immensely compared with that cooled by cryogenes. Compared with the conventional regenerative cryocoolers, pulse tube cryocooler is the best option for cooling optic systems, for it works without any moving component at the cold end. The wear-out in the cold finger of pulse tube cryocooler is eliminated, and the vibration as well as the electromagnetic interference at the cold end is substantially reduced. As a pulse tube cryocooler has long life time, high reliability, small mass, small size, and low vibration, it is used to cool the lens, as shown in Fig.6. The pulse tube cryocooler has a heat lift of 25 W at 150 K.



(a) Pulse tube cryocooler



(b) Cooling capacity of the cryocooler

Fig.6 Old source for the optical system

Because a lens can only be mounted by its edge, conduction heat transfer method which is applied to cool the lens can only occur through the edge. In this system, since the diameter of the pulse tube cryocooler's cold finger is 25 mm, if the cold head is connected directly to the 70 mm-diameter lens, large thermal gradient within the lens would be generated. Temperature difference in the lens would produce great stress which can break the lens, especially during the cooling down process. The heat transfer model of the lens cooled by a pulse tube cryocooler is built to optimize the thermal performance of the lens mount. The heat transfer path between the lens and cold finger is shown in Fig.7.

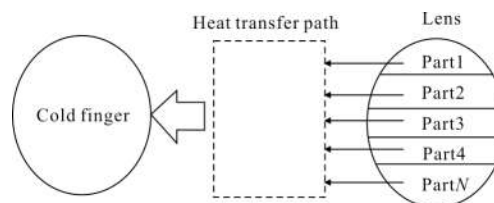


Fig.7 Heat transfer model between the lens and cold finger

The lens can be divided into  $N$  parts. The temperature of each part is respected as  $T_1, T_2, T_3 \dots T_N$  respectively. Heat transfer between the lens and the cold finger can be expressed as<sup>[14]</sup>:

$$Q=K \cdot A \frac{(T_C-T_N)}{L} \quad (6)$$

where  $K$  is the thermal conductivity,  $A$  is the cross-sectional area of the conductive structure,  $T_C$  is the cold head temperature, and  $T_N$  is the temperature of a part of the lens. It can be seen from the formula that when  $K, A,$  and  $T_C$  are constants, the temperature of each part can be obtained equal by making the heat transfer path of each part equivalent.

The model of lens directly cooled by the pulse tube cryocooler is shown in Fig.8(a).  $T_1$  and  $T_2$  are the temperature of the two points in the lens, and  $\Delta L$  is the heat transfer path difference between the two points. The heat transfer direction is respected by the arrow in the figure. According to Eq.(6), the temperature difference between the two points is calculated by:

$$\Delta T=T_1-T_2 \quad (7)$$

where

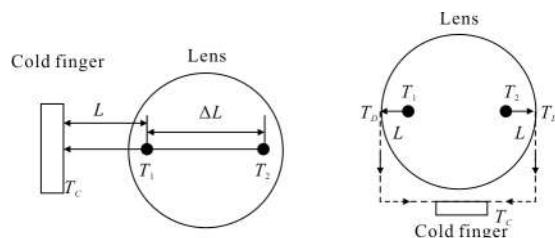
$$T_1=T_C-\frac{Q \cdot L}{K \cdot A} \quad (8)$$

$$T_2=T_C-\frac{Q \cdot (L+\Delta L)}{K \cdot A} \quad (9)$$

The temperature difference between the two points is  $\Delta T=Q \cdot \Delta L / K \cdot A$ . If the temperature difference is too large, thermal stress will be produced in the lens.

The optimized structure model is shown in Fig.8(b),  $T_1$  and  $T_2$  are in the same position as in Fig.8(a). The heat transfer path between the lens and the cold finger is changed from a single path to symmetrical double paths, as shown by the dotted lines in Fig.8(b). This path can be made of metal material with good thermal conductivity in order to reduce the temperature difference between  $T_C$  and  $T_D$ . Due to the same heat transfer

path between the two points, theoretically, there is no temperature difference between them. The optimized lens support structure will greatly improve the internal uniformity of the temperature distribution.



(a) Directly cooled model (b) Optimized model

Fig.8 Heat transfer path contrast

Under the guidance of this design concept, the thermal design of the support structure is shown in Fig.9. The heat transfer path between the lens and the cold finger has two equal paths. According to the above analysis, this structure is beneficial to ensure the temperature uniformity inside the lens during the cooling. A thermal strap is used to transfer heat from the optical components to the mechanical cooler.

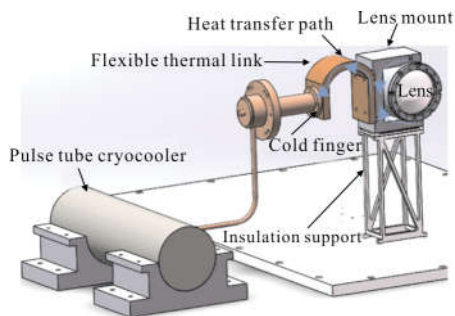
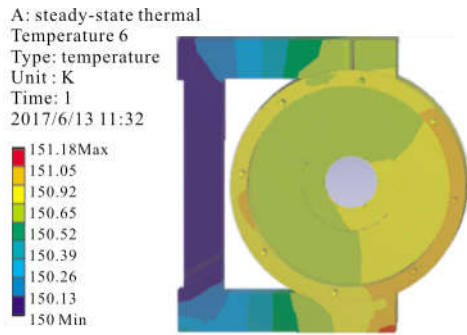
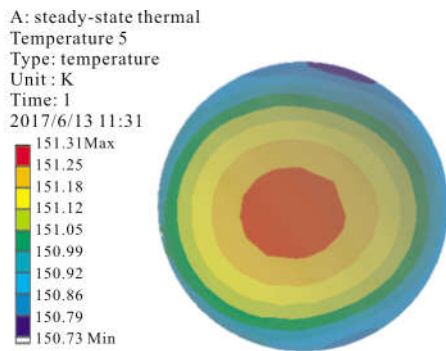


Fig.9 Lens mount thermal conduct structure

Prediction of the temperature gradient using ANSYS Workbench is shown in Fig.10. As this system works in the vacuum environment, the main contribution to the heat load is the radiation and conduction. The results of temperature contours of optical components show that the uniformity of the temperature field is less than 1 K. This low temperature difference will not lead to large thermal stress.



(a) Lens mount temperature



(b) Lens1 temperature

Fig.10 Thermal analysis of the lens mount

## 4 Test result

When the prototype lens mount was built, many tests were carried out to assess the thermal and mechanical behavior of the mount.

### 4.1 Lens mount thermal behavior test

To verify the temperature of the lens and the validity of the lens mount, the dedicated experiments have been conducted on a prototype optics. The photograph of the experimental setup is shown in Fig.11. The test setup system consists of lens cell, two pulse tube cryocoolers, a vacuum box, a blackbody and a detector. A flexible thermal strap was used to transfer the heat from lens to the pulse tube cryocooler. An insulation support was used to reduce conduction leakage as low as possible, multi-layer insulation screens were also used to reduce the radiation heat load from the vacuum box. Due to the large size of lens1, its temperature and thermal gradient were measured.

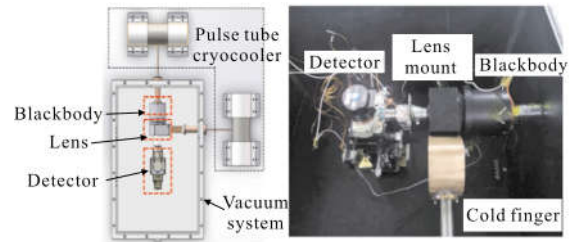


Fig.11 Structure of test system

The lens prototype was fixed inside the cryostat and twelve temperature sensors were fixed in different areas of the prototype and the cold base. When the pulse tube cryocoolers began to work, the lens started to be cooled down. During the cooling of the lens, temperatures across the lens element were monitored with ten PT100 resistance temperature sensors. Temperature monitoring sensors 2, 3, 4, 5 were attached to the first surface of the lens1, and sensors 7, 9, 10, 11 were attached to the second surface. Sensors 1 and 8 were attached to the center of surface1 and surface2 respectively. Sensors 6 and 12 were attached to the lens mount and the cold finger respectively.

The temperatures indicated by the different sensors during cooling down were plotted against time. The temperature of the cryogenic optical components successfully reached 150 K from the room temperature, as shown in Fig.12. It has taken about 3 hours to cool the optical components down because the cold mass to be cooled was about 850 g. Despite the lens working temperature required by this system was 150 K, the lens was

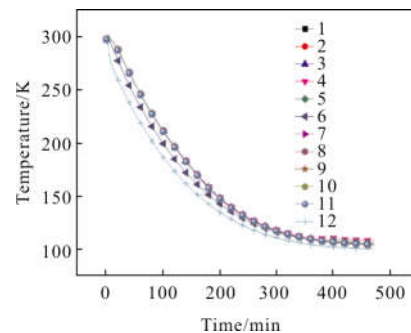


Fig.12 Temperature against time during cooldown



cooled to a lower temperature to study the effect of the mount on the lens in a wider temperature range. Finally, without the closed-loop temperature control of the mechanical cooler, the first lens was cooled down to 105 K and survived the test with no damage.

The radial temperature difference of surface1 as well as that of surface2 is represented by the value of surface temperature standard deviation. The temperature difference between sensors 1 and 8 represents the axial temperature difference. As the thermal radiation reaches surface1 first, the temperature of  $T_1$  is higher than  $T_8$ . The temperature difference across the lens is plotted against time, as shown in Fig.13. The temperature uniformity of both surface1 and surface2 is less than 0.2K, and the maximum temperature difference between sensors 1 and 8 is less than 1 K. This small temperature difference will not produce large thermal stress to damage the lens. In addition, it has little effect on the refractive index of the lens material, which ensures good image quality.

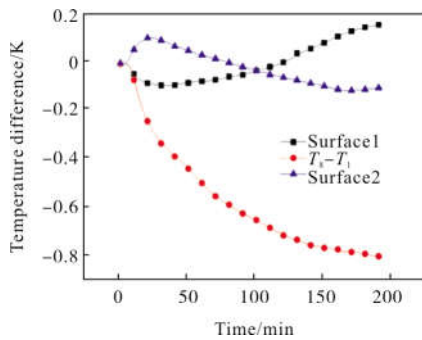


Fig.13 Temperature difference across the lens against time

#### 4.2 Lens mount mechanical behavior test

A test was also conducted to examine lens distortion caused by the mount distortion during the cooling process. As the laser interferometer was sensitive to vibration, another experimental device was designed, as shown in Fig.14. The test setup system consists of test lens, heat sink, insulation support, vacuum chamber, activated

carbon and window. The heat sink was cooled by liquid nitrogen. Activated carbon was used to maintain the vacuum environment required for the measurement.

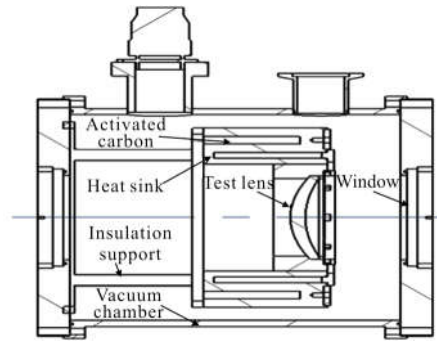


Fig.14 Structure of distortion test equipment

Since the large diameter of the lens1, the deformation will be the largest in the optical system, in this study only the lens1 is tested for deformation. After the lens was assembled into the mount by using the radial support and the axial support, the lens was cooled in a vacuum environment. As mentioned above, the lens can survive a temperature of 105 K under this support structure. In order to study the influence of the support structure on the lens in the wide temperature range, the lens temperature was reduced to 120 K with a predetermined safety margin. Once this was done, cooling and vacuum systems were stopped to reduce the vibration impactation on the measurement. Then, the lens distortion was examined under a Zygo interferometer, the test results were shown in Fig.15.

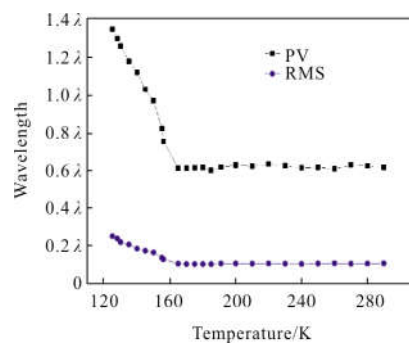


Fig.15 Lens distortion test results

It can be seen from the measurement results that the lens surface shape is stable in the temperature range of 165–300 K mainly because the lens barrel does not contact with the lens during the cooling process and no radial stress is developed. The deformation of the lens is mainly caused by the radial support and axial support preload. Within this temperature range, the force of the radial and axial support remains constant, hence the deformation of the mirror caused by the supports also maintains a constant value. In addition, the change of temperature can merely cause a change in the curvature of the sphere, but this change is not reflected in the PV and RMS values which describe the reference of surface deviation.

As the temperature is further reduced, the lens distortion becomes larger because the lens barrel contacts with the outer margin of the optic, which would cause radial force to be exerted upon the rim of the optic. This force compresses the optic radially and creates radial stress. As the temperature keeps decreasing, the stress gradually increases. The experimental temperature of lens barrel contacted with the lens is higher than the value of theoretical calculation. Because the inner margin of lens barrel is not ideal circle, during the cooling process, the smaller diameter part of the barrel contacts with the lens surface first. At the operation temperature of 150 K, the lens deformation PV value is  $0.97 \lambda$ , which is in good agreement with the theoretical analysis. The test results show that the designed support structure can well meet the needs of the cryogenic optical system.

## 5 Conclusions

In this paper, a novel-structure lens mount for the cryogenic optical system cooled by a pulse tube cryocooler is introduced. The validity of the

lens mount has been verified by experimental tests. The radial support and axial support are designed successfully to ensure the deformation less than 1 wave at cryogenic temperature with the advantages of simple and adjustable. A low temperature difference less than 1 K within the lens is achieved by establishing a double heat transfer paths with equal length between the cold finger and the lens. As the preload of the lens mount is adjustable, it can provide low-stress support for other cryogenic optics with different operation temperature. Also, the design methods of the lens mount in this paper are meaningful for the cases that mechanical cryocoolers are used to cool down the optical system. With the help of this lens mount, the possibility of using pulse tube cryocooler to cool the optics has also been verified, which is of great significance for the development of cryogenic optics.

## References:

- [1] Tian Qijie, Chang Songtao, He Fengyun, et al. Internal stray radiation measurement for cryogenic infrared imaging systems using a spherical mirror [J]. *Applied Optics*, 2017, 56(17): 4918–4925. (in Chinese)
- [2] Xia X L, Shuai Y, Tan H P. Calculation techniques with the Monte Carlo method in stray radiation evaluation [J]. *Journal of Quantitative Spectroscopy & Radiative Transfer*, 2005, 95(1): 101–111.
- [3] Pfisterer Richard N, Ellis K Scott, Pompea Stephen M. The role of stray light modeling and analysis in telescope system engineering, performance assessment and risk abatement[C]//SPIE, 2010, 7738: 320–330.
- [4] Park Jun-Oh, Jang Won Kweon, Kim Seonghui, et al. Stray light analysis of high resolution camera for a low-earth-orbit satellite [J]. *Journal of the Optical Society of Korea*, 2011, 15(1): 52–55.
- [5] Du Baolin, Li Lin, Huang Yifan. Stray light analysis of an on-axis three-reflection space optical system [J]. *Chinese Optics Letters*, 2010, 8(6): 569–572.
- [6] Baumeister H, Bizenberger P, Bailer-Jones C A L, et al.

- Cryogenic engineering for Omega2000: Design and performance [C]//SPIE, 2003, 4841: 343–354.
- [7] Thibault S, Vallee P, Artigau E. GPI –cryogenic spectrograph optics performances[C]//SPIE, 2010, 7735: 73551N.
- [8] Rohloff R R, Laun W, Graser U, et al. Cryo design for the VLT MIDI instrument [C]//SPIE, 2000, 4006: 277–288.
- [9] Thibault S. Recent development in cryogenic optical and mechanical design[C]//SPIE, 2013, 8720: 872009.
- [10] Greene Thomas, Beichman Charles, Gully –Santiago Michael, et al. NIRCам: development and testing of the JWST Near –Infrared camera [C]//SPIE, 2010, 7731: 77310C.
- [11] Kaneda H, Onaka T, Yamashiro R, et al. Optical performance of the ASTRO –F telescope at cryogenic temperatures[C] //SPIE, 2003, 4850: 230–240.
- [12] Paul R Yoder, Jr. Opto–mechanical System Design[M]. Beijing: China Machine Press, 2008. (in Chinese)
- [13] Moriaki Wakaki, Keiei Kudo, Takehisa Shibuya. Physical Properties and Data of Optical Materials[M]. Beijing: Chemical Industry Press, 2009. (in Chinese)
- [14] Yang Shiming, Tao Wenquan. Heat Transfer [M]. Beijing: Higher Education Press, 2008. (in Chinese)